

## An Unusual H<sub>2</sub> Sorption Mechanism in PCN-14: Insights From Molecular Simulation

Tony Pham,<sup>†,§</sup> Katherine A. Forrest,<sup>†,§</sup> and Brian Space<sup>\*,†</sup>

<sup>†</sup>*Department of Chemistry, University of South Florida,  
4202 East Fowler Avenue, CHE205, Tampa, FL 33620-5250, United States*

<sup>§</sup>Authors contributed equally

\*brian.b.space@gmail.com

### Repulsion/Dispersion and Polarizability Parameters

For simulations of H<sub>2</sub> sorption in PCN-14, repulsion/dispersion interactions were calculated using the Lennard-Jones 12–6 potential, which is the following:<sup>1</sup>

$$U_{LJ} = 4\epsilon_{ij} \left[ \left( \frac{\sigma_{ij}}{r_{ij}} \right)^{12} - \left( \frac{\sigma_{ij}}{r_{ij}} \right)^6 \right] \quad (1)$$

where  $r_{ij}$  is the distance between sites  $i$  and  $j$ ,  $\epsilon_{ij}$  is the depth of the potential well between sites  $i$  and  $j$ , and  $\sigma_{ij}$  is the distance between sites  $i$  and  $j$  at which  $U_{LJ} = 0$ . The Lennard-Jones parameters for all MOF atoms were taken from the Universal Force Field (UFF).<sup>2</sup> The interactions between unlike species were calculated using the Lorentz–Bertholet mixing rules, which are the following:<sup>3</sup>

$$\epsilon_{ij} = (\epsilon_{ii}\epsilon_{jj})^{\frac{1}{2}} \quad (2)$$

$$\sigma_{ij} = \frac{1}{2}(\sigma_{ii} + \sigma_{jj}) \quad (3)$$

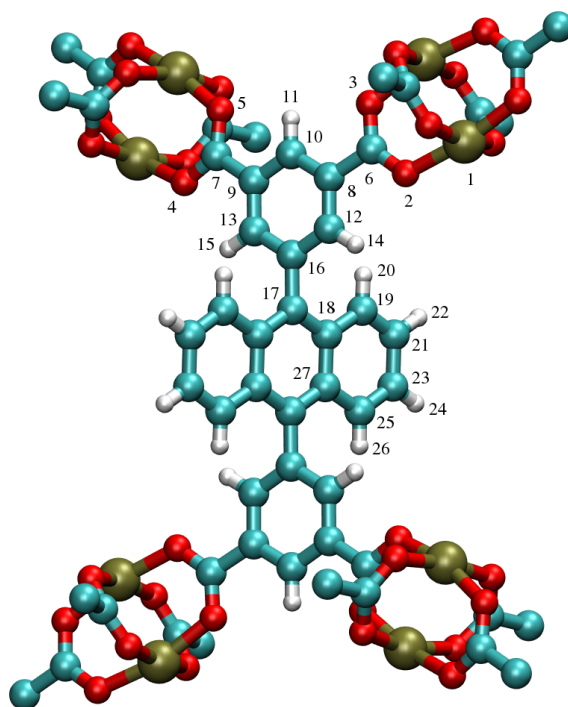
For simulations including explicit many-body polarization, atomic point polarizabilities were assigned to the nuclear center of all atoms of PCN-14. The exponential damping-type polarizabilities for all C, H, and O atoms were taken from a highly transferable set provided by the work of van Duijnen and Swart.<sup>4</sup> The polarizability parameter for Cu<sup>2+</sup> was determined in previous work<sup>5</sup> and used herein. The many-body polarization energy of the MOF–H<sub>2</sub> system was calculated using a Thole–Applequist type model.<sup>6–9</sup> The repulsion/dispersion and polarizability parameters that were used for all MOF atoms for the simulations in this work are provided in Table S1.

**Table S1.** Lennard–Jones  $\epsilon$  and  $\sigma$  and atomic point polarizability ( $\alpha^\circ$ ) parameters used for the C, H, O, and Cu atoms for the simulations in this work.

| Atom | $\epsilon$ (K) | $\sigma$ (Å) | $\alpha^\circ$ (Å <sup>3</sup> ) |
|------|----------------|--------------|----------------------------------|
| C    | 52.84000       | 3.43100      | 1.28860                          |
| H    | 22.14000       | 2.57100      | 0.41380                          |
| O    | 30.19000       | 3.11800      | 0.85200                          |
| Cu   | 2.51600        | 3.11400      | 2.19630                          |

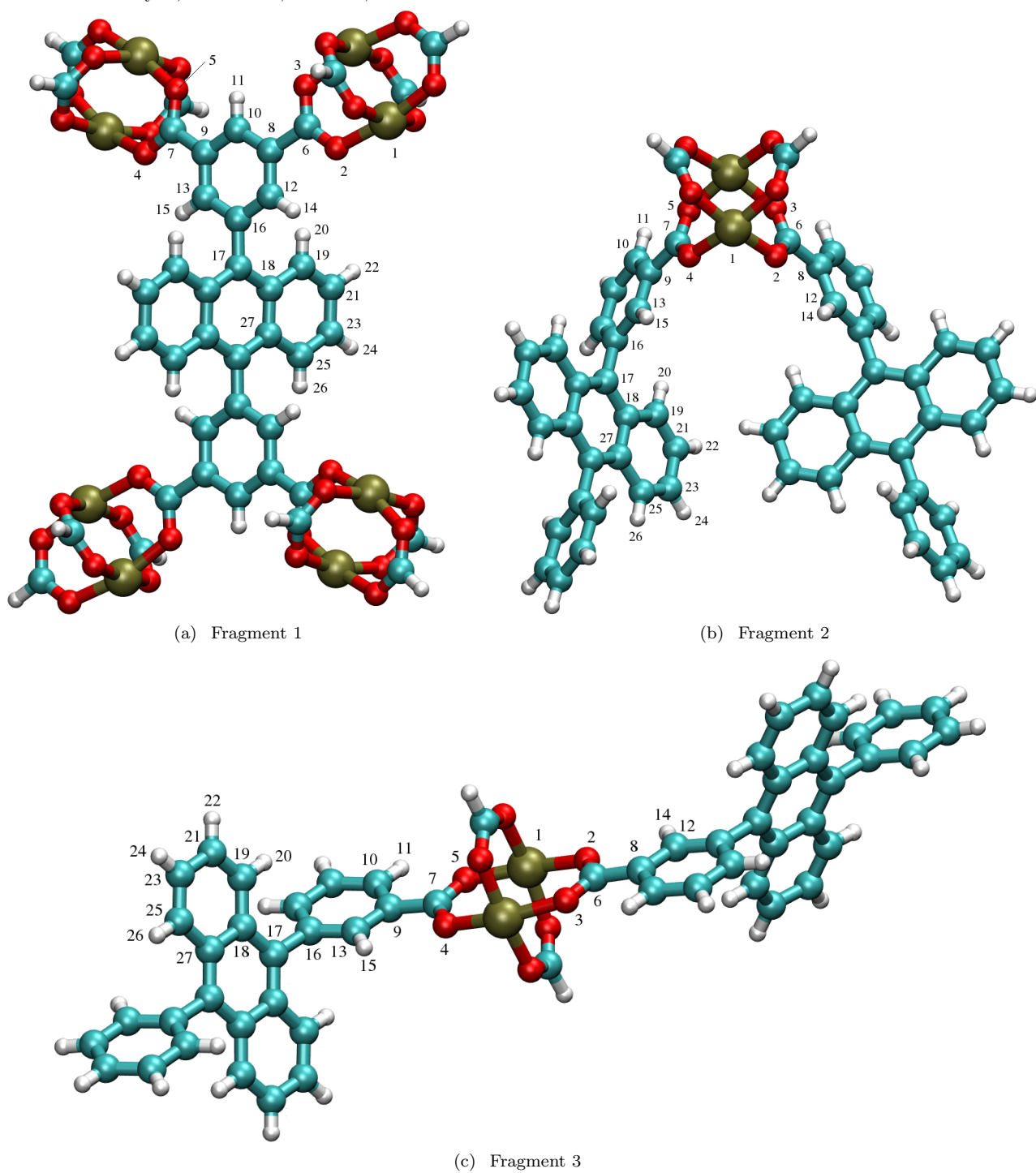
## Electronic Structure Calculations

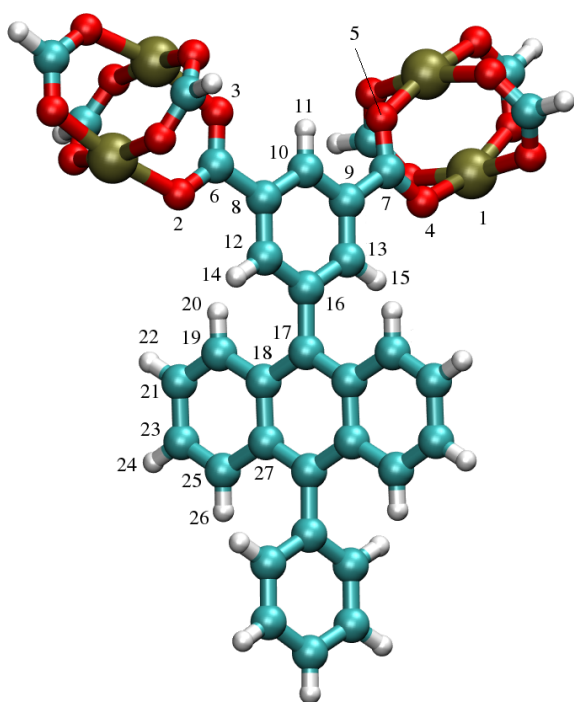
The partial charges for the various chemically distinct atoms in PCN-14 (Figure S1) were determined through electronic structure calculations on different fragments that were taken from the crystal structure of the MOF. The five fragments that were considered for PCN-14 in this work are shown in Figure S2. The NWChem *ab initio* simulation software<sup>10</sup> was used to calculate the electrostatic potential surface (ESP) of the considered fragments. For these calculations, all C, H, and O atoms were treated with the 6-31G\* basis set to produce overpolarized charges that are appropriate for condensed phase simulation,<sup>11</sup> while the LANL2DZ ECP basis set<sup>12-14</sup> was assigned to the Cu<sup>2+</sup> ions for proper treatment of the inner electrons of this species. The CHELPG method<sup>15,16</sup> was used to fit the charges onto the atomic centers of each fragment to reproduce the respective ESPs. The calculated average partial charges for each chemically distinct atom within the fragments are provided in Table S2. Note, atoms that are located on the edges of the fragment were not included in the averaging. The partial charges for all chemically distinct atoms were averaged between the fragments. The partial charges were then adjusted so that the total charge of the framework was neutral. The final tabulated results for each chemically distinct atom in PCN-14 can be found in Table S3.



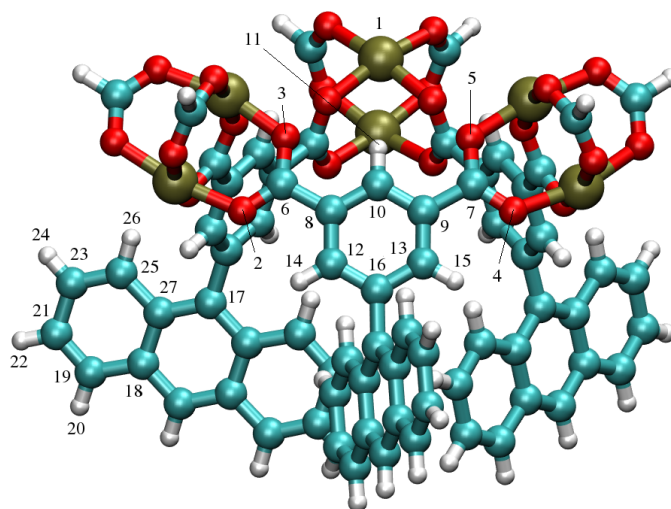
**Figure S1.** The numbering of the chemically distinct atoms in PCN-14 as referred to in Tables S2 and S3. Atom colors: C = cyan, H = white, O = red, Cu = tan.

**Figure S2.** Fragments of PCN-14 that were selected for gas phase charge fitting calculations. Label of atoms correspond to Figure S1. Atom colors: C = cyan, H = white, O = red, Cu = tan.





(d) Fragment 4



(e) Fragment 5

**Table S2.** Calculated average partial charges ( $e^-$ ) for the various chemically distinct atoms for the fragments that were selected for PCN-14. Labeling of atoms and fragments correspond to Figures S1 and S2, respectively.

| Atom | Label | Fragment 1 | Fragment 2 | Fragment 3 | Fragment 4 | Fragment 5 |
|------|-------|------------|------------|------------|------------|------------|
| Cu   | 1     | 1.1610     | 1.0327     | 0.9887     | 1.1594     | 1.0860     |
| O    | 2     | -0.7497    | -0.7609    | -0.6859    | -0.7664    | -0.7416    |
| O    | 3     | -0.7855    | -0.7301    | -0.6737    | -0.7820    | -0.7615    |
| O    | 4     | -0.7886    | -0.7195    | -0.6879    | -0.7760    | -0.7317    |
| O    | 5     | -0.7853    | -0.7042    | -0.7049    | -0.7782    | -0.7625    |
| C    | 6     | 1.0279     | 1.0404     | 0.9663     | 1.0290     | 0.9968     |
| C    | 7     | 1.0428     | 0.9520     | 0.9999     | 1.0468     | 0.9962     |
| C    | 8     | -0.1685    | -0.1436    | -0.1734    | -0.1577    | -0.1681    |
| C    | 9     | -0.1653    | -0.1462    | -0.1802    | -0.1707    | -0.1671    |
| C    | 10    | -0.1599    | -0.1667    | -0.1183    | -0.1522    | -0.1449    |
| H    | 11    | 0.2356     | 0.1791     | 0.1678     | 0.2251     | 0.2227     |
| C    | 12    | -0.1804    | -0.2395    | -0.2067    | -0.2544    | -0.1927    |
| C    | 13    | -0.1756    | -0.1926    | -0.1979    | -0.2076    | -0.1777    |
| H    | 14    | 0.1689     | 0.1667     | 0.1519     | 0.2001     | 0.1777     |
| H    | 15    | 0.1719     | 0.1425     | 0.1458     | 0.1828     | 0.1664     |
| C    | 16    | 0.3686     | 0.3940     | 0.3794     | 0.4654     | 0.3923     |
| C    | 17    | -0.2747    | -0.2751    | -0.2744    | -0.2982    | -0.3476    |
| C    | 18    | 0.1261     | 0.0867     | 0.1195     | 0.1156     | 0.1129     |
| C    | 19    | -0.1804    | -0.1889    | -0.2183    | -0.2352    | -0.1931    |
| H    | 20    | 0.1056     | 0.1236     | 0.1284     | 0.1306     | 0.1238     |
| C    | 21    | -0.1027    | -0.1177    | -0.0978    | -0.0794    | -0.0987    |
| H    | 22    | 0.1294     | 0.1234     | 0.1215     | 0.1229     | 0.1152     |
| C    | 23    | -0.1289    | -0.1039    | -0.1116    | -0.1251    | -0.0893    |
| H    | 24    | 0.1364     | 0.1237     | 0.1225     | 0.1344     | 0.1196     |
| C    | 25    | -0.1520    | -0.1859    | -0.1793    | -0.1931    | -0.2246    |
| H    | 26    | 0.0997     | 0.1054     | 0.1076     | 0.1094     | 0.1276     |
| C    | 27    | 0.0825     | 0.1302     | 0.1009     | 0.1267     | 0.1675     |

**Table S3.** The partial charges ( $e^-$ ) for the chemically distinct atoms in PCN-14 that were used for the simulations in this work. Label of atoms correspond to Figure S1.

| Atom | Label | $q$ ( $e^-$ ) |
|------|-------|---------------|
| Cu   | 1     | 1.08320       |
| O    | 2     | -0.74090      |
| O    | 3     | -0.74660      |
| O    | 4     | -0.74070      |
| O    | 5     | -0.74700      |
| C    | 6     | 1.01000       |
| C    | 7     | 1.00540       |
| C    | 8     | -0.16220      |
| C    | 9     | -0.16590      |
| C    | 10    | -0.14840      |
| H    | 11    | 0.20570       |
| C    | 12    | -0.21470      |
| C    | 13    | -0.19030      |
| H    | 14    | 0.17270       |
| H    | 15    | 0.16160       |
| C    | 16    | 0.39910       |
| C    | 17    | -0.29400      |
| C    | 18    | 0.11190       |
| C    | 19    | -0.20310      |
| H    | 20    | 0.12210       |
| C    | 21    | -0.09920      |
| H    | 22    | 0.12220       |
| C    | 23    | -0.11170      |
| H    | 24    | 0.12700       |
| C    | 25    | -0.18700      |
| H    | 26    | 0.10960       |
| C    | 27    | 0.12120       |

### Grand Canonical Monte Carlo

Simulations of H<sub>2</sub> sorption in PCN-14 were performed using grand canonical Monte Carlo (GCMC) on a single unit cell of the MOF. This method involves keeping the chemical potential ( $\mu$ ), volume ( $V$ ), and temperature ( $T$ ) of a simulation box consisting of the MOF-H<sub>2</sub> system to be constant while allowing the particle number ( $N$ ) and other statistical mechanical variables to fluctuate.<sup>17</sup> The H<sub>2</sub> molecules were randomly inserted, deleted, translated, or rotated within the simulation box based on a random number generator. Periodic boundary conditions were applied in order to approximate a macroscopic MOF environment. A spherical cutoff corresponding to half the shortest unit cell dimension length was used for the simulations. The average particle number,  $\langle N \rangle$ , was calculated by the following expression:<sup>18,19</sup>

$$\langle N \rangle = \frac{1}{\Xi} \sum_{N=0}^{\infty} e^{\beta\mu N} \left\{ \prod_{i=1}^{3N} \int_{-\infty}^{\infty} dx_i \right\} N e^{-\beta U_{FH}(x_1, \dots, x_{3N})} \quad (4)$$

where  $\Xi$  is the grand canonical partition function,  $\beta$  is equal to the quantity  $1/kT$  ( $k$  is the Boltzmann constant),  $\mu$  is the chemical potential of the gas reservoir, and  $U_{FH}$  is the potential energy of the MOF-H<sub>2</sub> system that accounts for fourth order Feynman-Hibbs quantum corrections.  $\mu$  for H<sub>2</sub> was determined for a range of temperatures and pressures using the BACK equation of state.<sup>20</sup> The Feynman-Hibbs corrections were applied to the total potential energy,  $U$ , according to the following equation:<sup>21</sup>

$$U_{FH} = U + \frac{\beta\hbar^2}{24\mu_m} \left( U'' + \frac{2}{r} U' \right) + \frac{\beta^2\hbar^4}{1152\mu_m^2} \left( \frac{15}{r^3} U' + \frac{4}{r} U''' + U'''' \right) \quad (5)$$

where  $\hbar$  is the reduced Planck's constant,  $\mu_m$  is the reduced mass, and the primes indicate differentiation with respect to pair separation  $r$ .  $U$  represents the sum of the repulsion/dispersion energy (equation 1), the electrostatic energy as calculated through Ewald summation,<sup>22,23</sup> and the many-body polarization energy as calculated using a Thole-Applequist type model.<sup>6-9</sup>

The excess H<sub>2</sub> uptake, defined as the amount of H<sub>2</sub> sorbed in the pore volume of the MOF in excess of the bulk gas capacity in the same free space,<sup>24</sup> was determined from a calculation that utilized an experimental pore volume ( $V_p$ ) of 0.87 cm<sup>3</sup> g<sup>-1</sup> for PCN-14<sup>25</sup> and bulk gas densities ( $\rho_b$ ) *via* the following expression:

$$R_{ex} = \frac{1000m(\langle N \rangle - V_p\rho_b)}{M} \quad (6)$$

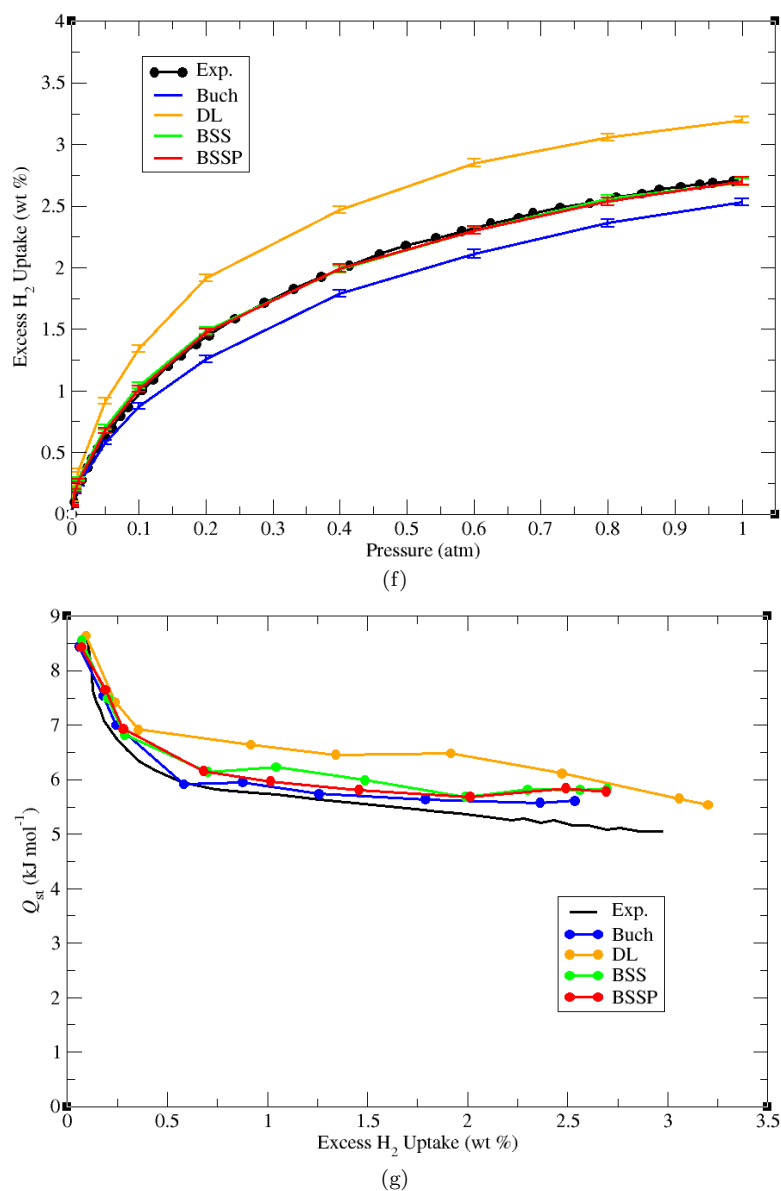
where  $m$  is the molar mass of the sorbate and  $M$  is the molar mass of the MOF. The excess weight percent ( $wt\%_{ex}$ ) of H<sub>2</sub> sorbed in PCN-14 was calculated by:

$$wt\%_{ex} = \frac{100R_{ex}}{1000 + R_{ex}} \quad (7)$$

The simulated isosteric heat of adsorption ( $Q_{st}$ ) values were calculated based on fluctuations in  $N$  and  $U$  in the MOF-H<sub>2</sub> system through the following expression:<sup>26</sup>

$$Q_{st} = -\frac{\langle NU \rangle - \langle N \rangle \langle U \rangle}{\langle N^2 \rangle - \langle N \rangle^2} + kT \quad (8)$$

For all state points considered, the simulations initially consisted of  $1 \times 10^6$  Monte Carlo (MC) steps to reach equilibrium. The simulations continued for an additional  $2 \times 10^6$  MC steps to sample the desired thermodynamic properties. The simulations were decorrelated by sampling every  $1 \times 10^3$  MC steps. All simulations were performed using the Massively Parallel Monte Carlo (MPMC) code,<sup>27</sup> which is currently available for download on GitHub.

Simulated H<sub>2</sub> Sorption Results

**Figure S3.** (a) Low-pressure (up to 1.0 atm) excess H<sub>2</sub> sorption isotherms in PCN-14 at 77 K for experiment (black) and simulations using the Buch (blue),<sup>28</sup> DL (orange),<sup>29</sup> BSS (green),<sup>30</sup> and BSSP (red) models.<sup>30</sup> (b) Isosteric heats of adsorption ( $Q_{st}$ ) for H<sub>2</sub> in PCN-14 plotted against H<sub>2</sub> uptakes. The experimental data were estimated from reference 31.

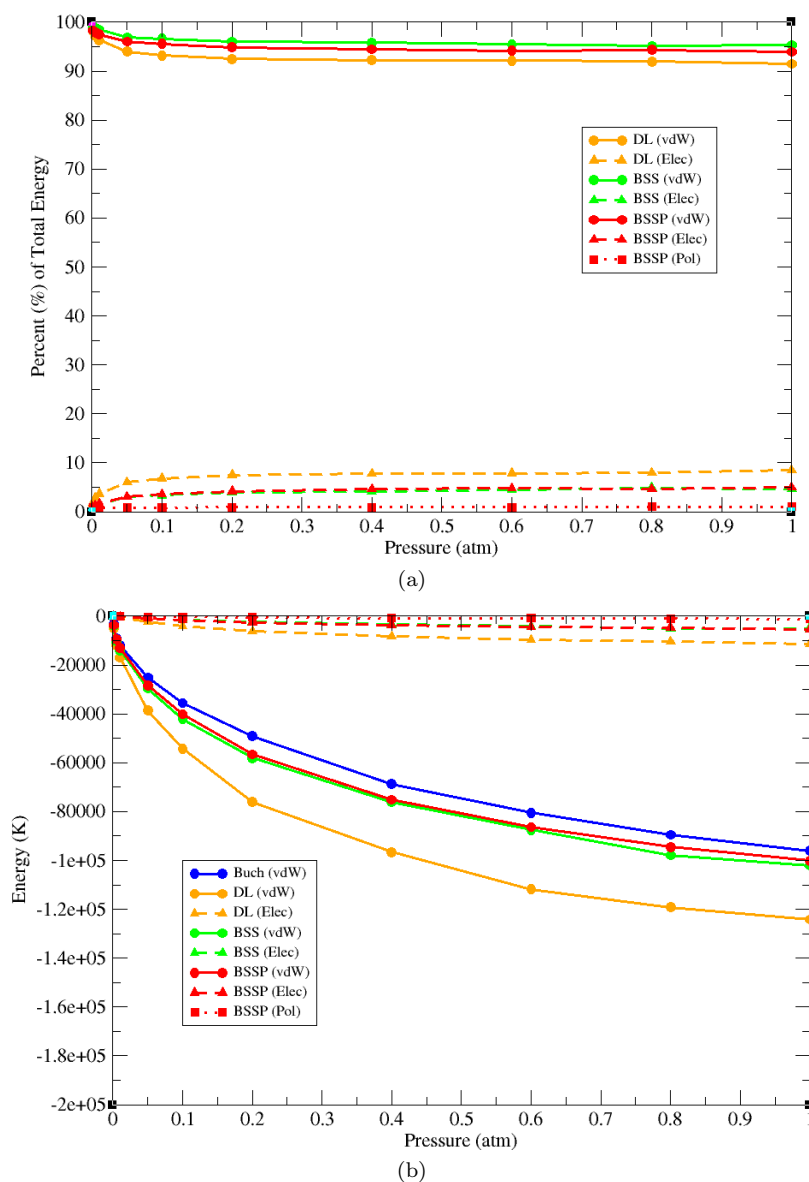


**Figure S4.** Energy decomposition per H<sub>2</sub> molecule in PCN-14 at 77 K and pressures up to 1.0 atm for simulations using the Buch (blue),<sup>28</sup> DL (orange),<sup>29</sup> BSS (green),<sup>30</sup> and BSSP (red) models.<sup>30</sup> (a) shows the percent contribution of energy components, while (b) shows the absolute energy magnitudes in units of K. Line type indicates the energy component with solid lines with circles corresponding to van der Waals (vdW) contributions, dashed lines with triangles corresponding to electrostatic (Elec) contributions, and dotted lines with squares corresponding to polarization (Pol) contributions.

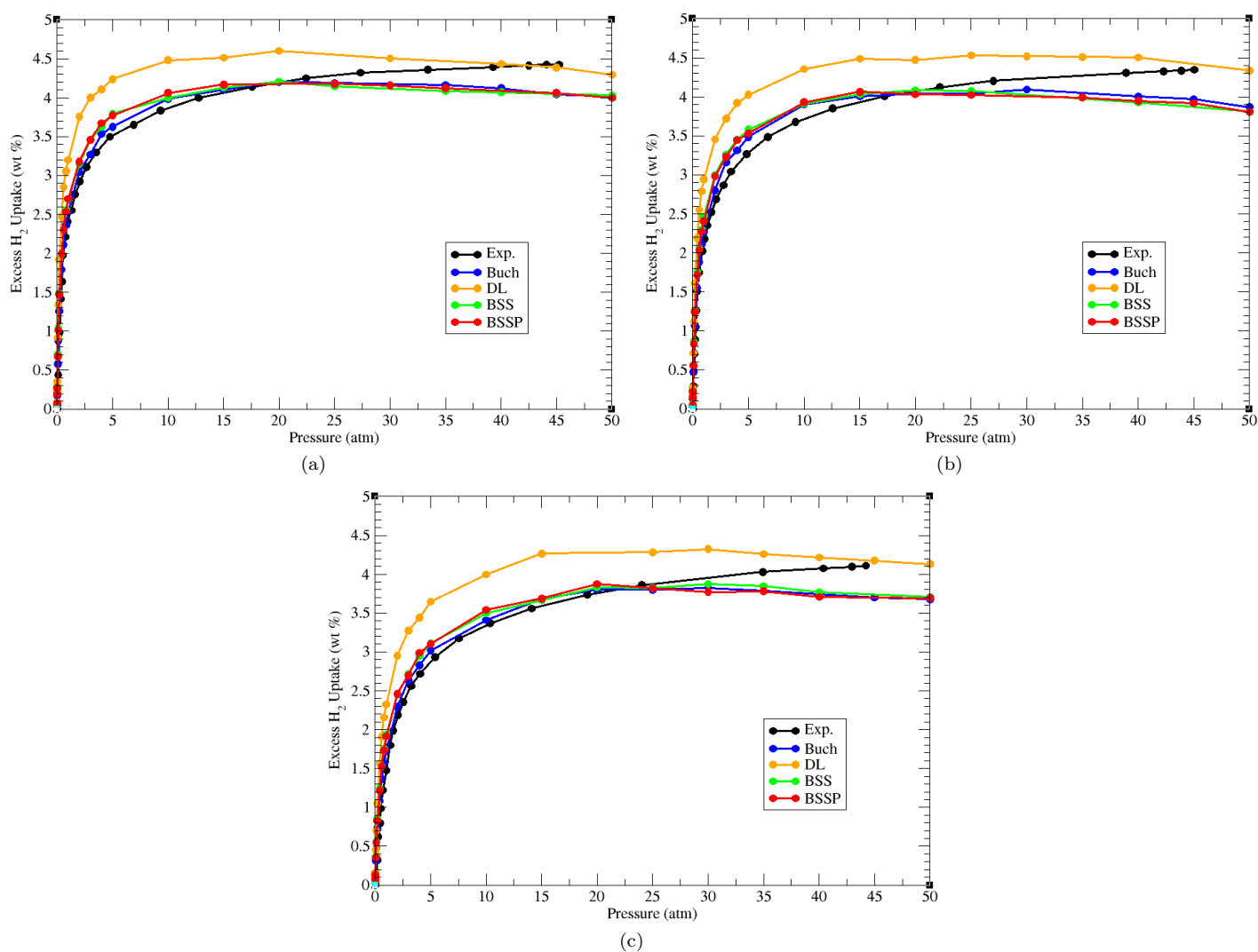


**Figure S5.** High-pressure (up to 50.0 atm) excess  $\text{H}_2$  sorption isotherms in PCN-14 at (a) 77 K, (b) 80 K, and (c) 87 K for experiment (black) and simulations using the Buch (blue),<sup>28</sup> DL (orange),<sup>29</sup> BSS (green),<sup>30</sup> and BSSP (red) models.<sup>30</sup> All experimental data were estimated from reference 31.

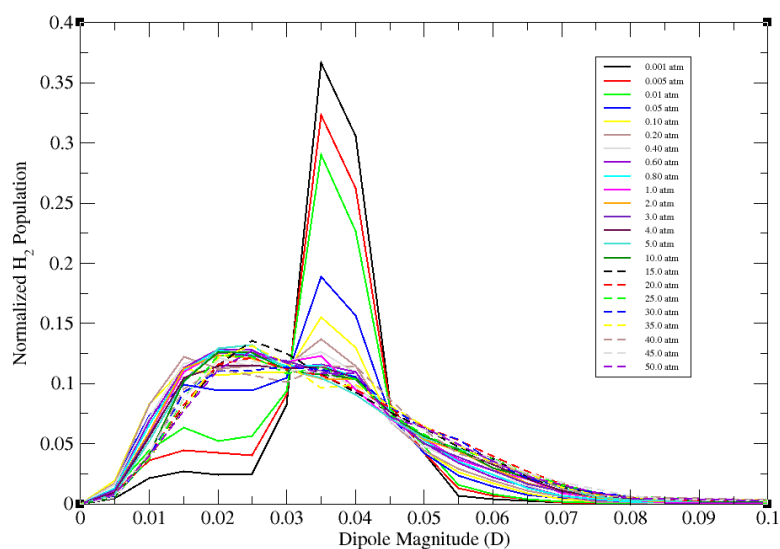


**Figure S6.** The normalized distribution of the induced dipoles on the sorbed  $\text{H}_2$  molecules for simulations using the BSSP model<sup>30</sup> in PCN-14 at 77 K and various pressures from 0.001 to 50.0 atm.

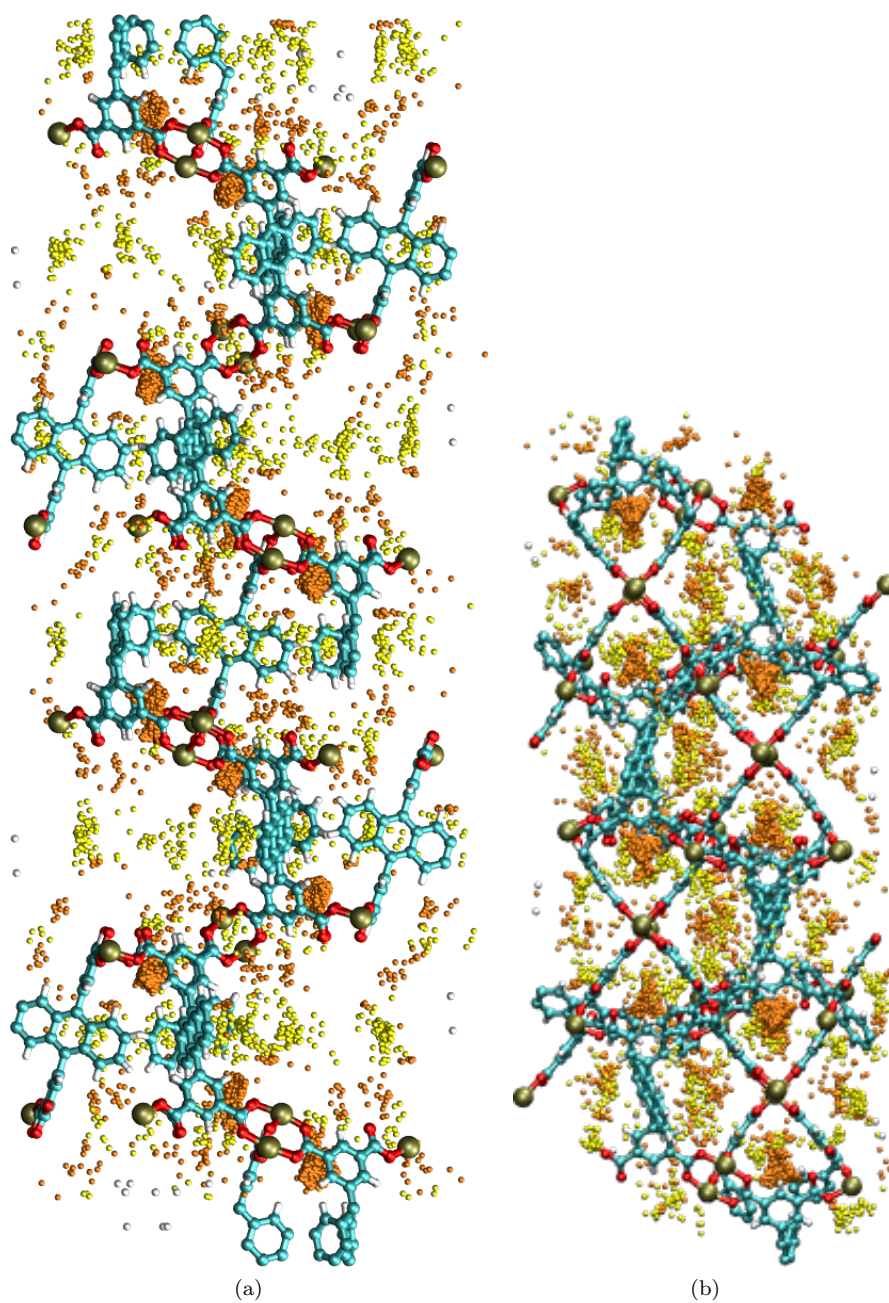


**Figure S7.** The orthographic view of (a) the  $29^\circ$  angle between the  $a$  and  $b$  axes and (b) the  $45^\circ$  angle between the  $b$  and  $c$  axes of the unit cell of PCN-14 showing the sites of  $\text{H}_2$  occupancy corresponding to the induced dipole magnitudes shown in Figure S6. Orange-colored occupancy correspond to  $\text{H}_2$  molecules with induced dipoles of 0.30 D and above, while yellow-colored occupancy correspond to  $\text{H}_2$  molecules with induced dipoles of 0.00 to 0.30 D. Atom colors: C = cyan, H = white, O = red, Cu = tan.

- 
- <sup>1</sup> J. Jones, *Proc. R. Soc. London, Ser. A*, 1924, **106**, 463–477.
  - <sup>2</sup> A. K. Rappé, C. J. Casewit, K. S. Colwell, W. A. Goddard and W. M. Skiff, *J. Am. Chem. Soc.*, 1992, **114**, 10024–10035.
  - <sup>3</sup> M. P. Allen and D. J. Tildesley, *Computer Simulation of Liquids*, Oxford University Press, Oxford, United Kingdom, 1989.
  - <sup>4</sup> P. T. van Duijnen and M. Swart, *J. Phys. Chem. A*, 1998, **102**, 2399–2407.
  - <sup>5</sup> K. A. Forrest, T. Pham, K. McLaughlin, J. L. Belof, A. C. Stern, M. J. Zaworotko and B. Space, *J. Phys. Chem. C*, 2012, **116**, 15538–15549.
  - <sup>6</sup> J. Applequist, J. R. Carl and K.-K. Fung, *J. Am. Chem. Soc.*, 1972, **94**, 2952–2960.
  - <sup>7</sup> B. Thole, *Chem. Phys.*, 1981, **59**, 341–350.
  - <sup>8</sup> K. A. Bode and J. Applequist, *J. Phys. Chem.*, 1996, **100**, 17820–17824.
  - <sup>9</sup> K. McLaughlin, C. R. Cioce, T. Pham, J. L. Belof and B. Space, *J. Chem. Phys.*, 2013, **139**, 184112.
  - <sup>10</sup> M. Valiev, E. Bylaska, N. Govind, K. Kowalski, T. Straatsma, H. V. Dam, D. Wang, J. Nieplocha, E. Apra, T. Windus and W. de Jong, *Comput. Phys. Commun.*, 2010, **181**, 1477–1489.
  - <sup>11</sup> W. D. Cornell, P. Cieplak, C. I. Bayly, I. R. Gould, K. M. Merz, D. M. Ferguson, D. C. Spellmeyer, T. Fox, J. W. Caldwell and P. A. Kollman, *J. Am. Chem. Soc.*, 1995, **117**, 5179–5197.
  - <sup>12</sup> W. J. Stevens, H. Basch and M. Krauss, *J. Chem. Phys.*, 1984, **81**, 6026–6033.
  - <sup>13</sup> P. J. Hay and W. R. Wadt, *J. Chem. Phys.*, 1985, **82**, 270–283.
  - <sup>14</sup> L. A. LaJohn, P. A. Christiansen, R. B. Ross, T. Atashroo and W. C. Ermler, *J. Chem. Phys.*, 1987, **87**, 2812–2824.
  - <sup>15</sup> L. E. Chirlian and M. M. Francl, *J. Comput. Chem.*, 1987, **8**, 894–905.
  - <sup>16</sup> C. M. Breneman and K. B. Wiberg, *J. Comput. Chem.*, 1990, **11**, 361–373.
  - <sup>17</sup> N. Metropolis, A. W. Rosenbluth, M. N. Rosenbluth, A. H. Teller and E. Teller, *J. Chem. Phys.*, 1953, **21**, 1087–1092.
  - <sup>18</sup> D. A. McQuarrie, *Statistical Mechanics*, University Science Books, Sausalito, CA, 2000.
  - <sup>19</sup> D. Frenkel and B. Smit, *Understanding Molecular Simulation: From Algorithms to Applications*, Academic Press, New York, 2002.
  - <sup>20</sup> T. Boublík, *Fluid Phase Equilib.*, 2005, **240**, 96–100.
  - <sup>21</sup> R. P. Feynman and A. R. Hibbs, *Quantum Mechanics and Path Integrals*, McGraw-Hill, New York, 1965.
  - <sup>22</sup> P. P. Ewald, *Ann. Phys.*, 1921, **369**, 253–287.
  - <sup>23</sup> B. A. Wells and A. L. Chaffee, *J. Chem. Theory Comput.*, 2015, **11**, 3684–3695.
  - <sup>24</sup> A. L. Myers and P. A. Monson, *Langmuir*, 2002, **18**, 10261–10273.
  - <sup>25</sup> S. Ma, D. Sun, J. M. Simmons, C. D. Collier, D. Yuan and H.-C. Zhou, *J. Am. Chem. Soc.*, 2008, **130**, 1012–1016.
  - <sup>26</sup> D. Nicholson and N. G. Parsonage, *Computer Simulation and the Statistical Mechanics of Adsorption*, Academic Press, London, 1982.
  - <sup>27</sup> J. L. Belof and B. Space, *Massively Parallel Monte Carlo (MPMC)*, Available on GitHub, 2012, <https://github.com/mpmccode/mpmc>.
  - <sup>28</sup> V. Buch, *J. Chem. Phys.*, 1994, **100**, 7610–7629.
  - <sup>29</sup> F. Darkrim and D. Levesque, *J. Chem. Phys.*, 1998, **109**, 4981–4984.
  - <sup>30</sup> J. L. Belof, A. C. Stern and B. Space, *J. Chem. Theory Comput.*, 2008, **4**, 1332–1337.
  - <sup>31</sup> S. Ma, J. M. Simmons, D. Sun, D. Yuan and H.-C. Zhou, *Inorg. Chem.*, 2009, **48**, 5263–5268.